

Effect of some thiophene derivatives on the electrochemical behavior of AISI 316 austenitic stainless steel in acidic solutions containing chloride ions

II. Effect of temperature and surface studies

A. Galal*, N.F. Atta, M.H.S. Al-Hassan

Department of Chemistry, College of Science, University of Cairo, Giza, Egypt

Received 4 July 2004; received in revised form 10 August 2004; accepted 24 August 2004

Abstract

The temperature coefficient of 2-thiophene carboxylic hydrazide (TCH) at austenitic stainless steel of type 316 (AISI 316) was determined in an acid medium in the temperature range 20–40 °C. The corrosion rate increases with temperature with an inhibition efficiency that ranges between 89 and 99%. The inhibitor forms a surface layer at the metal substrate. Evidence of the formation of the surface layer was confirmed from surface reflectance infrared spectroscopy measurements. The elemental composition of the surface as indicated from energy-dispersive X-ray analysis and X-ray photoelectron spectroscopy (XPS) proved that the application of the inhibitor increases the concentration of Cr at the surface of the specimen. The adsorption model for this inhibitor follows a Langmuir isotherm and the heat of adsorption indicates a chemical bond formation. The latter was confirmed from the XPS data that indicated the possible formation of a chemical bond between the sulfur atom of the inhibitor molecule and the metal substrate. Scanning electron microscopy was used to study the surface morphology before and after exposure to the inhibitor.

© 2004 Elsevier B.V. All rights reserved.

Keywords: Electrochemistry; Corrosion; Stainless steel; Thiophene derivatives; Temperature coefficient; Surface reflectance

1. Introduction

Organic compounds and their derivatives were used successfully as inhibitors for different types of steels and were studied extensively through the last century. Recently, interest is still growing for exploiting other inhibitors for the corrosion of stainless steels [1]. On the other hand, type 316 stainless steel (AISI 316) has a wide scope of applications in different industries [2]. This type of stainless steel is covered with a protective film rich in chromium (oxides/hydroxides) that imparts corrosion resistance to its surface. However, chloride-containing acidic solutions are aggressive to this film layer and results in severe pitting forma-

tion. Several organic molecules contain sulfur and nitrogen hetero-atoms were suggested as inhibitors for steel in acidic medium [3]. The inhibition mechanism for this class of inhibitors is mainly based on adsorption [4]. On the other hand, the effect of some inhibitors on chloride-ion-induced pitting of stainless steels was reported in the literature [5] to follow a pattern consistent with Galvele's pit model [6]. Among the few publications cited in the literature on the effect of temperature on the inhibitive action is that using some benzotriazoles to inhibit the corrosion of type 304 stainless steel [7]. In their study, the authors [7] showed that the mercaptobenzotriazoles inhibited the corrosion of stainless steel at temperatures between 25 and 50 °C using a chemisorption model.

In the first part of this work [8], we studied the effect of some thiophene derivatives on the electrochemical behavior

* Corresponding author. Tel.: +20 782 5266; fax: +20 568 5799.
E-mail address: galalah1@yahoo.com (A. Galal).

of AISI 316 austenitic stainless steel in acidic solutions containing chloride ions. We found a correlation between the molecular structure of these derivatives and their inhibition efficiency. The aim of this part of the study was to determine the temperature coefficient and the adsorption characteristics of one of the thiophene derivatives, namely, 2-thiophene carboxylic hydrazide (TCH). Moreover, we investigated the surface morphology of the steel before and after inhibitor application and its adsorption onto the surface of the substrate. The surface structure of the steel is investigated and related to the adsorption of the inhibitor onto the substrate surface.

2. Experimental details

AISI 316 stainless steel chemical composition and other chemicals used in this study are as described elsewhere [8]. Test solutions were prepared from stock and diluted using de-ionized water supply, further details can be found in previous work [8].

AISI 316 stainless steel specimens were in the form of rods and sheets. The first type was used for the electrochemical experiments while the sheets were employed for the surface measurements. Electrode mounting and preparation were as previously described [8]. Flat sheets were mounted to a glass cell in the form of a cylinder, mounted with a chemical resistant rubber seal in contact with the flat specimens. The surface preparation of the flat sheets electrode followed the same procedure as described for the rod samples. The working electrode geometrical surface area was 5.2 cm^2 . A three-electrode one-compartment glass cell with a saturated Ag/AgCl reference electrode and a platinum sheet ($2 \text{ cm} \times 2 \text{ cm}$) counter electrode was used for all the electrochemical measurements.

Electrochemical equipments and conditions of measurements are as described earlier [8].

The surface morphology of the specimen was characterized using scanning electron microscopy (SEM) and energy-dispersive X-ray analyzer (EDAX) Jeol JSM-5600 model. The adsorption of the organic molecule to the substrate was examined using surface reflectance Fourier transform infrared spectroscopy (FT-IR). X-ray photoelectron spectroscopy (XPS) was used to examine the elemental composition of the surface.

The samples were coated with a thin film of gold to eliminate the effect of charging during measurements. A Jeol JFC-1200 fine coater was used for this purpose and a current of 20 mA was applied for 150 s coating period. A Perkin-Elmer ESCA-5300 spectrometer was used to obtain the spectra of the chemical composition of the surface of the steel samples. A pass energy of 25 eV was used and the energy scale was adjusted to read the Au $4f_{7/2}$ peak at 83.8 eV. The sample charging effect was corrected relative to the carbon peak energy of atmospheric hydrocarbons at 284.6 eV.

3. Results and discussion

3.1. Temperature coefficient of corrosion inhibition of stainless steel by 2-thiophene carboxylic hydrazide

The corrosion of stainless steel 316 in 0.5 M H_2SO_4 in absence and presence of different concentrations of TCH (ca. 5.0×10^{-4} to 1.0×10^{-2} M) at different temperatures ($25\text{--}40^\circ\text{C}$) was studied using Tafel and linear polarization experiments. The inhibition efficiency was calculated as previously described [8].

Fig. 1 shows the plot of the protection efficiency against the logarithm of concentration of TCH at different temperatures. The data reveal that the extent of efficiency increases with the concentration of the inhibitor as mentioned before. On the other hand, it was found that the inhibition efficiency decreases with increasing temperature. General irregularity could be observed at some concentrations for different temperatures. The studied inhibitor is a five-member heterocyclic ring with either half-chair or envelope-like structures [9,10] with the most probable structure in the half-chair form. The adsorption may be mainly via the lone-pair of the sulfur atom in the ring while the rest of the molecule covers the surface in the case of TCH. Some interaction of the electron cloud of the ring could also be expected along with water displacement from the surface as indicated previously by Ren and Hubbard [11]. The resulting mode of coverage of the inhibitor to the

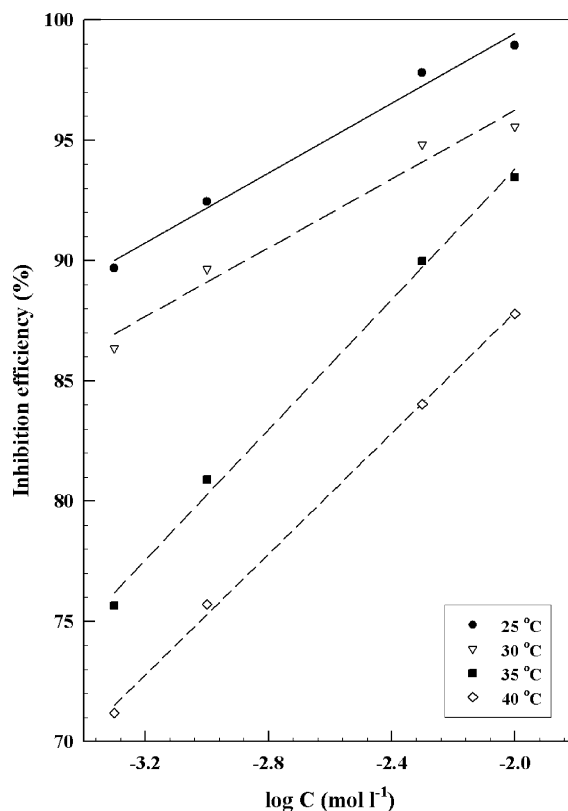


Fig. 1. Inhibition efficiency for different concentration of TCH at different temperatures.

surface would be an anchor (through the sulfur atom) and a blanket (from the rest of the molecule). Different adsorption isotherms were suggested in the literatures [10–12] and were tested for their fit to the experimental data. The degree of coverage, θ , at constant potential is given by the following relation [13,14]:

$$\theta = 1 - \frac{i_c}{i_a} \quad (1)$$

where i_a and i_c are the corrosion currents of uninhibited and inhibited experiments, respectively. As was indicated above, the inhibition efficiency increases with concentration, however some irregularities are clear at some concentrations with temperature as shown in Fig. 1. The latter is confirmed by inspecting the values of the Tafel constants listed in Table 1. More interestingly, the values of the cathodic Tafel constant (β_c) that corresponds to hydrogen evolution in absence of inhibitor, decreased noticeably as the temperature increases from 25 to 30 °C. The value of β_c starts to increase again as the temperature increases above 30 °C. Bockris and Drazis [15] formalized a mechanism for the hydrogen evolution reaction as β_c decreases with temperature. In this case, the mechanism seems to work similarly for lower temperatures and changes as the temperature increases. On the other hand, the corresponding values of β_a showed a similar trend as those for β_c . The relatively lower values found in this study for the stainless steel compared to those found for mild steel [16] and iron [17], are due to less impurities present in stainless steel. The inhibition efficiency is, therefore, more pronounced at lower temperatures. The calculated protection efficiencies when using 5.0×10^{-3} M TCH are 77.2, 56.0, 51.7, 57.9% in 0.5 M H_2SO_4 at 25, 30, 35, and 40 °C, respectively. The values of inhibition efficiencies calculated from the linear polarization measurements are comparable to those estimated from the Tafel experiments. Other researchers mentioned similar findings earlier [18–20].

At this stage, we are assuming that a layer of the thiophene inhibitor adsorbs onto the surface of the stainless steel. This later finding is confirmed by the surface reflectance FT-IR measurements shown in a later section. Therefore, the fraction of the surface covered by the inhibitor and not exposed to corrosion events is equivalent to $(i_a - i_c/i_a)$. The latter assumption is only valid when complete coverage of the surface by the inhibitor is readily maintained at all temperature ranges studied.

Moreover, the curves possess characteristic s-shaped isotherms for some temperatures and concentration regions of the acid used that indicated an adsorption mechanism for the inhibition process. Thus, Fig. 2 shows the Langmuir adsorption isotherm relation given by the following equation [16]:

$$\frac{\theta}{1 - \theta} = AC \exp\left(\frac{Q}{RT}\right) \quad (2)$$

where A is a constant, C the inhibitor concentration, Q the heat of adsorption, θ the part of surface covered by the in-

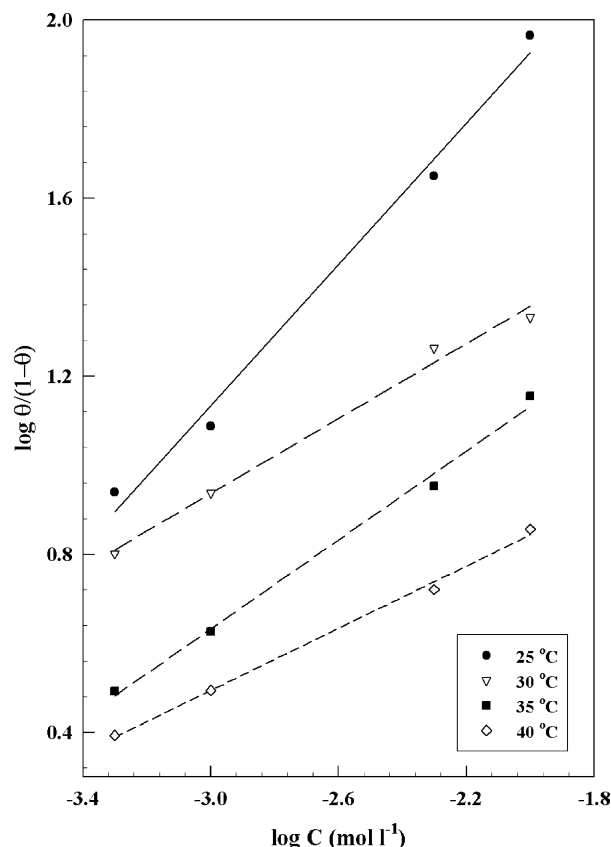


Fig. 2. Adsorption isotherm of TCH for the different concentrations of inhibitor studied at different temperatures.

hibitor, $(1 - \theta)$ the fraction of the vacant sites, R the gas constant, and T the absolute temperature. A plot of $\log[\theta/(1 - \theta)]$ versus $\log C$ should yield a straight line. As could be noticed from Fig. 2 that as the temperature reaches 40 °C, the change in surface coverage at relatively high temperature differs in magnitude and extent when compared to lower temperatures. A plot of $\log[\theta/(1 - \theta)]$ versus $1/T$ at given concentration values (Fig. 3) allows to estimate the heats of adsorption: -129.7 , -68.48 , -82.47 and -57.67 $K \text{ mol}^{-1}$ for 5.0×10^{-4} , 1.0×10^{-3} , 5.0×10^{-3} and 1.0×10^{-2} M inhibitor, respectively. On the other hand, the heat of adsorption could be estimated from the relation between the rate of corrosion and the inverse of temperature [16]. In this method, the total measured rate of corrosion could be expressed as the sum of two rates, the first for the rate of uninhibited reaction, and the second for the rate of corrosion of completely covered surface. The expression for these two rates is [16]:

$$\frac{-d[\text{Fe}]}{dt} = K_1(1 - \theta) + K_2\theta \quad (3)$$

where K_1 and K_2 are the rate constants of the two processes, respectively.

In most of our discussion, we will be considering the Langmuir model of adsorption. Thus, from substituting for the

Table 1

Electrochemical parameters for stainless steel of type 316 in 0.5 M H₂SO₄ in the absence and presence of different concentrations of 2-thiophene carboxylic hydrazide from Tafel experiments

<i>T</i> (°C)	Inhibitor (mol l ⁻¹)	<i>E</i> _{cor} (mV)	<i>β</i> _c (mV decade ⁻¹)	<i>β</i> _a (mV decade ⁻¹)	<i>R</i> _p (10 ² Ω cm ²)	<i>I</i> _{corr} (10 ⁻⁴ A cm ⁻²)	Corrosion rate (MPY)
25	0	-390	130	135	0.79	3.8	351
	5 × 10 ⁻⁴	-341	97	41	2.8	0.39	36.2
	1 × 10 ⁻³	-369	89	45	3.3	0.29	26.5
	5 × 10 ⁻³	-340	81	32	17	0.083	7.68
	1 × 10 ⁻²	-331	79	39	32	0.041	3.76
30	0	-334	81	43	1.2	4.0	367
	5 × 10 ⁻⁴	-338	94	40	2.6	0.54	50.1
	1 × 10 ⁻³	-319	91	35	3.2	0.41	38.0
	5 × 10 ⁻³	-292	106	24	3.8	0.21	19.0
	1 × 10 ⁻²	-284	98	31	8.0	0.18	16.3
35	0	-351	96	58	1.2	4.0	371
	5 × 10 ⁻⁴	-329	101	47	1.4	0.98	90.4
	1 × 10 ⁻³	-320	86	36	3.8	0.77	70.9
	5 × 10 ⁻³	-305	94	28	2.2	0.40	37.2
	1 × 10 ⁻²	-282	100	24	5.6	0.26	24.3
40	0	-342	114	89	0.93	4.2	388
	5 × 10 ⁻⁴	-804	93	37	1.2	1.2	112
	1 × 10 ⁻³	-802	96	36	1.4	1.0	94.2
	5 × 10 ⁻³	-305	94	43	2.1	0.67	61.9
	1 × 10 ⁻²	-296	84	37	2.9	0.51	47.4

values of θ from Eq. (2) into Eq. (3), we obtain:

$$\frac{-d[\text{Fe}]}{dt} = \frac{K_1 + K_2 AC \exp(Q/RT)}{1 + AC \exp(Q/RT)} \quad (4)$$

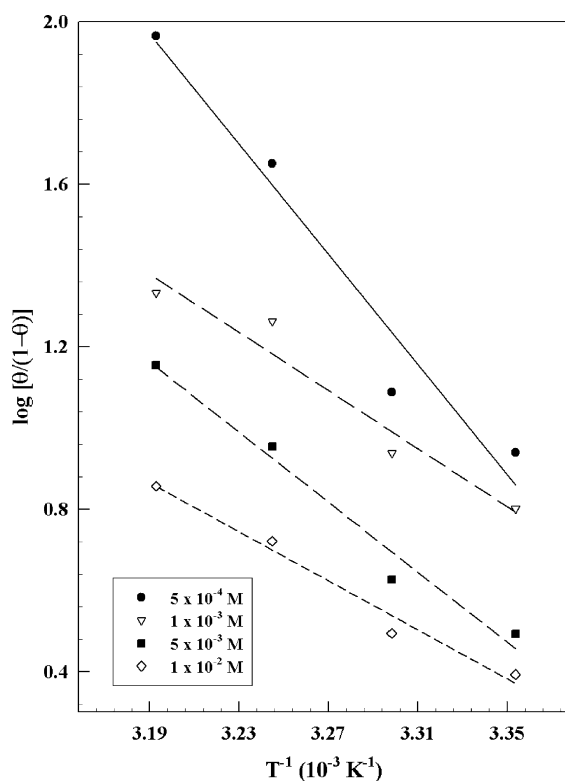


Fig. 3. Plot of $\log[\theta/(1-\theta)]$ vs. $1/T$ for given concentration values of TCH at stainless steel of type 316.

Therefore, the activation energy Q should increase as the extent of inhibition increases. This is related to the term $AC \exp(Q/RT)$, and when the surface is inhibited, C is equal to zero. Upon rearrangement of Eq. (4), where K_1 and K_2 are replaced by their exponential forms:

$$\frac{-d[\text{Fe}]}{dt} = \frac{K'_1 \exp(-E_1/RT) + K'_2 AC \exp[(Q - E_2)/RT]}{1 + AC \exp(-Q/RT)} \quad (5)$$

In the latter case, the activation energy for the corrosion process should be equal to E_1 . Moreover, as the extent of inhibition increases, and θ becomes large, the activation energy increases to equal $(E_1 + Q)$. At very large values for θ the activation energy is equal to E_2 . If we assume intermediate coverage by the inhibitor to the stainless steel surface and adopting the Langmuir model, the activation energy of adsorption can be determined. A plot of the rate of corrosion versus $1/T$ as in Fig. 4 allows the calculation of the activation energy of adsorption. The activation energy is then plotted versus the inhibitor concentration as shown in Fig. 5. The maximum value shown in Fig. 5 corresponds to the value of $(E_1 + Q)$ that is equal to 83.4 kJ mol^{-1} for $6.3 \times 10^{-3} \text{ mol}$. If E_1 for the uninhibited reaction is equal to $17.73 \text{ kJ mol}^{-1}$ [21], the heat of adsorption is equal to $65.67 \text{ kJ mol}^{-1}$. This value is reasonably agreeing with that obtained previously from the expression of Eq. (2).

From the aforementioned discussion, we can conclude that the inhibitor molecules are well adsorbed over the metal surface and that surface coverage of the stainless steel surface by the inhibitor changes with temperature and concentration, respectively. In the case of lack of interaction between adsorbed inhibitor molecules at the surface, the Langmuir model

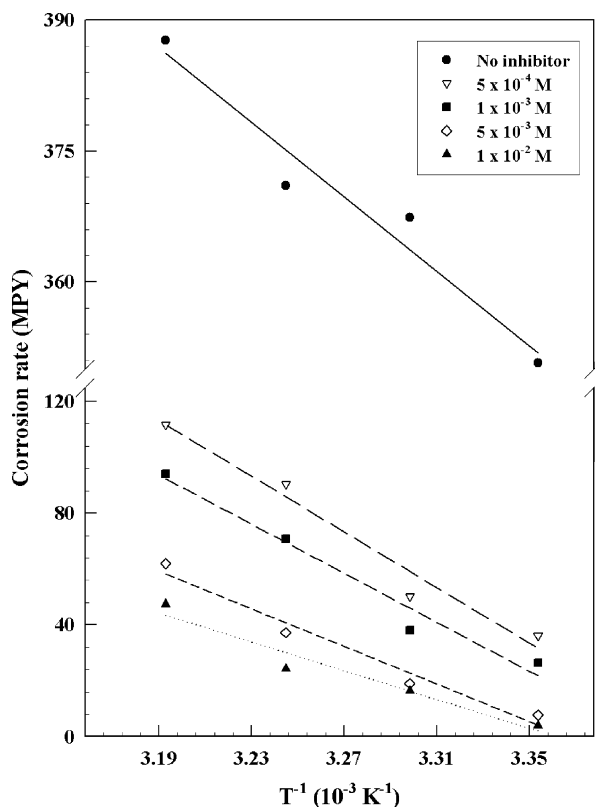


Fig. 4. Relation between the rate of corrosion of stainless steel of type 316 in H_2SO_4 vs. $1/T$; MPY (milli-inch per year) $\approx 0.00219 \text{ mA cm}^{-2}$.

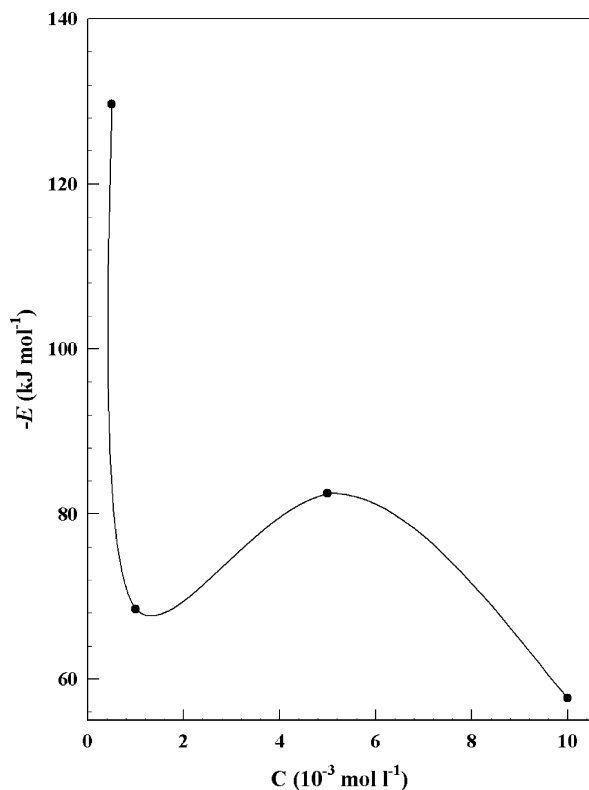


Fig. 5. Activation energy vs. inhibitor concentration.

Table 2
Thermodynamic parameters for TCH at the stainless steel surface in 0.5 M H_2SO_4

T ($^{\circ}C$)	ΔG_T° (kJ mol^{-1})	ΔH_T° (kJ mol^{-1})	ΔS_T° ($\text{J mol}^{-1} \text{K}^{-1}$)	dE/dT (V K^{-1})
30	-26.6	-38.6	-39.7	-2.05×10^{-7}
40	-26.2	-38.6	-39.7	-2.05×10^{-7}

suggests:

$$KC = \left[\frac{\theta}{1 - \theta} \right] \quad (6)$$

On the other hand, the thermodynamic parameters shown in Table 2 were estimated from the following relations [16]:

$$\Delta G_T^{\circ} = -RT \ln(K \times 55.5),$$

$$\Delta H_T^{\circ} = \frac{R(T_1 T_2 / (T_2 - T_1)) \ln K(T_2)}{K(T_1)},$$

$$\Delta S_T^{\circ} = \frac{\Delta H_T^{\circ} - \Delta G_T^{\circ}}{T} \quad (7)$$

And the temperature coefficient could be estimated according to:

$$\Delta G^{\circ} = \Delta H^{\circ} - ZFT \left(\frac{dE}{dT} \right) \quad (8)$$

$$E_{\text{eff}} = -2.3 \times 8.314 \times \frac{d \log i}{d \log(1/T)} \quad (9)$$

The enthalpy of adsorption, ΔH° , entropy of adsorption, ΔS° , and Gibbs energy of adsorption, ΔG° , are all negative (see Table 2). The negative value of ΔH° indicates the adsorption process is exothermic. On the other hand, the magnitude of ΔS° and ΔG° indicates that a replacement process took place during the adsorption of the inhibitor molecules at the surface of the stainless steel [22].

3.2. Surface measurements

3.2.1. Scanning electron microscopy

Fig. 6a and b shows the surface features of AISI 316 stainless steel exposed to 0.5 M H_2SO_4 in presence and absence of TCH for 10 min under potential step polarization conditions (the potential of the electrode was kept constant at -0.5 V for 60 s then stepped to a value of $+1.5 \text{ V}$ and held at this value for 600 s). Fig. 6a shows extensive corrosion in 0.5 M H_2SO_4 . Fig. 6b depicts the effect of adding $1.0 \times 10^{-3} \text{ M}$ TCH to 0.5 M H_2SO_4 on the surface characteristics of stainless steel under the same polarization conditions. The specimen surface is nearly intact as even the original polishing scratches are seen after the exposure. On the other hand, few pits are visible on the specimen surface after exposure to a 0.01 M NaCl-containing 0.5 M H_2SO_4 in absence and presence of inhibitor as shown in Fig. 7a and b, respectively.

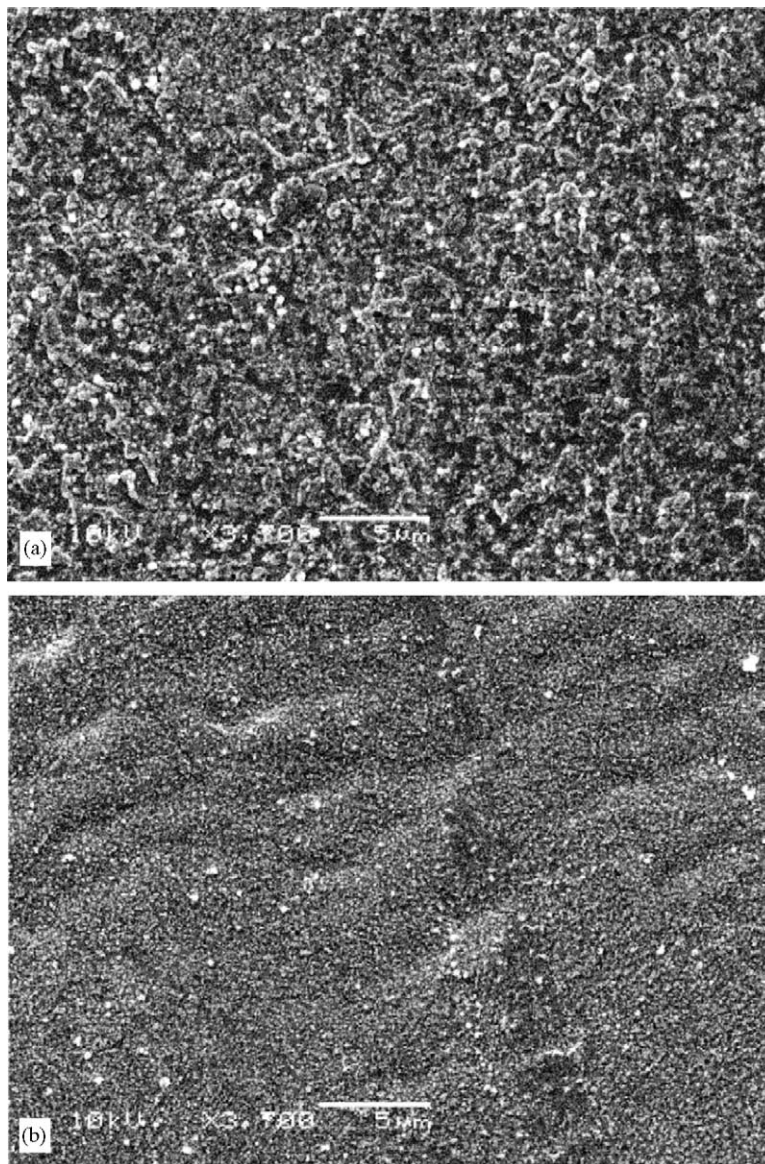


Fig. 6. SEM images showing surface features of stainless steel 316 exposed to 0.5 M H_2SO_4 in absence (a) and presence (b) of 1.0×10^{-3} M TCH for 10 min under potential step polarization conditions.

Energy-dispersive X-ray analysis (EDAX) was performed on the exposed stainless steel samples. The data are shown in Fig. 8a and b for a sample exposed to 0.5 M H_2SO_4 and to 0.5 M $\text{H}_2\text{SO}_4 + 1.0 \times 10^{-3}$ M TCH, respectively. Several important observations could be noticed from the data:

- (i) The general features of the spectra are similar in both cases, where the stainless steel is only exposed to the sulfuric acid solution and that containing the inhibitor.
- (ii) The amount of iron, nickel and molybdenum were affected when comparing the two graphs. Thus, the amount of iron, nickel and molybdenum decreased in the case of the sample exposed to inhibitor-containing solution, whereas the amount of chromium increases.

- (iii) A sulfur peak clearly appeared in the case of the sample exposed to the TCH.

The decrease in the amount of iron, nickel and molybdenum and the increase in the amount of chromium indicated that the dissolution of stainless steel is inhibited. Moreover, the appearance of the sulfur peak could be attributed to the adsorption of TCH moiety at the stainless steel surface. This assumption was confirmed by the data obtained from the FT-IR measurements.

3.2.2. Surface reflectance FT-IR

Surface reflectance FT-IR experiments were conducted on specimens that were exposed to 0.5 M H_2SO_4 and compared to stainless steel sheets exposed to 0.5 M $\text{H}_2\text{SO}_4 + 1.0 \times$

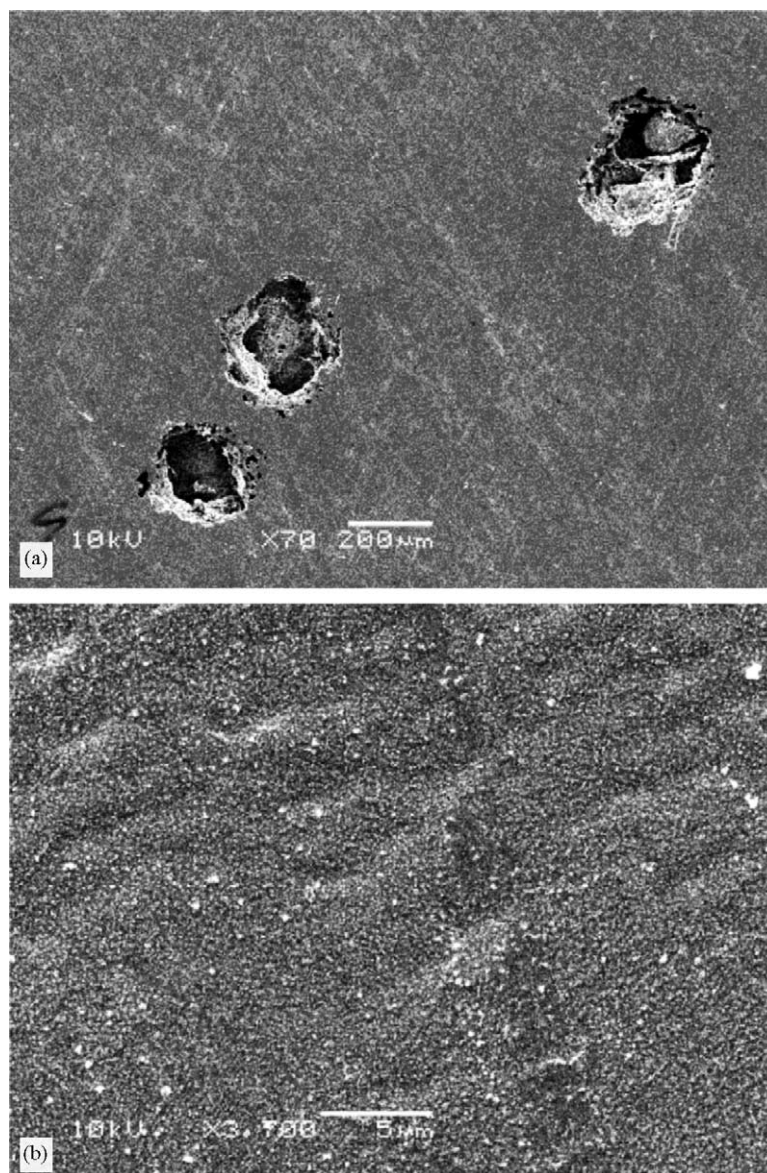


Fig. 7. SEM images of the specimen surface after exposure to a 0.01 M NaCl-containing 0.5 M H₂SO₄ in absence (a) and presence (b) of inhibitor.

10⁻³ M TCH. One important goal for this experiment was to ensure whether the inhibitor adsorbs to the surface of the metal substrate after exposure and thorough washing. Thus, Fig. 9 shows the spectrum obtained by reflectance from the surface of the stainless steel (a) and that obtained from a conventional transmission experiment of the TCH 2-thiophene carboxylic hydrazide (b). Region A is characterized by a strong “two-band” signal in the range 3100–500 cm⁻¹ that is characteristic of primary amines stretch [23]. Regions B and C are characteristic for the aromatic C–H stretch and bending bands of the thiophene ring at 1414 and 1075 cm⁻¹, respectively. A rather weak band appeared at 1660 cm⁻¹ that is thought to be due to the carbonyl group in the amide linkage –C=O–NH. At this stage, we can conclude that the inhibitor is adsorbed to the surface of the substrate via the

thiophene sulfur electron lone-pair, and those of the oxygen and the nitrogen atoms of the amide link. The presence of a thin oxide layer at the surface of the stainless steel is inevitable as indicated in the SEM images (Figs. 6 and 7) and from the X-ray photoelectron spectroscopy (XPS) data.

3.2.3. X-ray photoelectron spectroscopy

XPS data of stainless steel samples exposed to the inhibitor proved interaction between the inhibitor and the substrate are shown in Fig. 10. Thus, two S1 peaks appeared at down field, ca. 164.0 and 169.0 eV, cf. Fig. 10a in the case of inhibitor examined at the stainless steel surface versus one peak for the same compound at a platinum substrate cf. Fig. 10b. We suggest the formation of a metal–S bonding between inhibitor

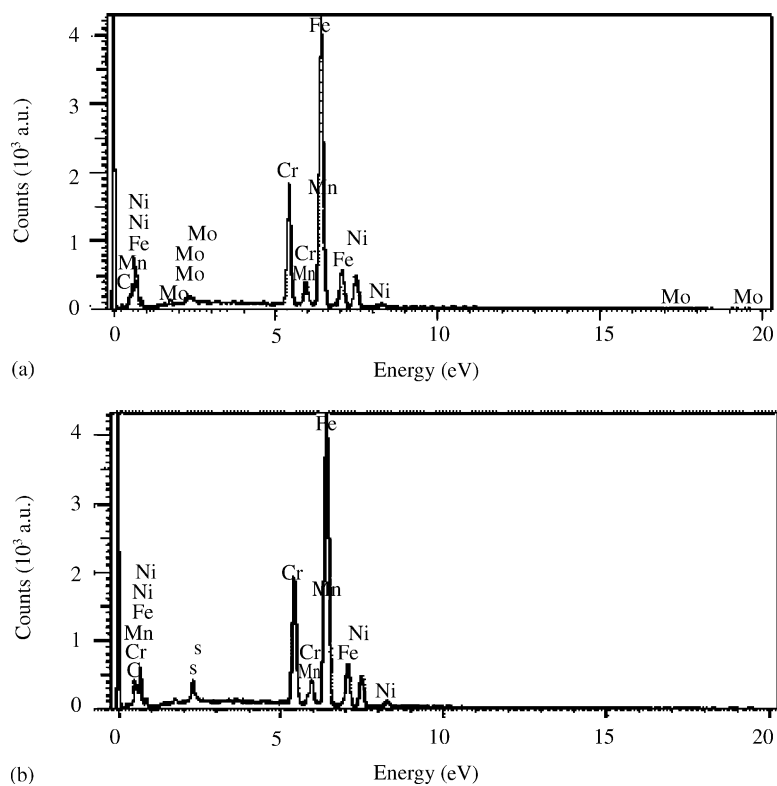


Fig. 8. Energy-dispersive X-ray analysis of the steel samples exposed to 0.5 M H₂SO₄ (a) and 0.5 M H₂SO₄ + 1.0 × 10⁻³ M TCH (b).

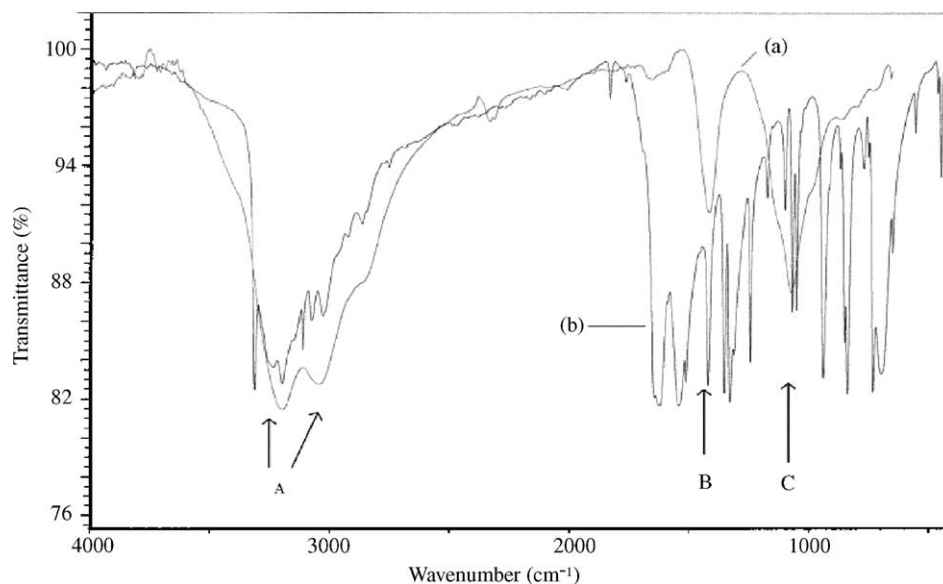


Fig. 9. FT-IR obtained by reflectance from the surface of the steel (a) and from a conventional transmission experiment (b) of TCH.

Table 3

Elemental composition (in wt.%) of the surface of steel before and after exposure to TCH in 0.5 M H₂SO₄

	Cr	Mn	Fe	Ni	Mo	S
Uninhibited	17.80	1.70	67.37	11.37	1.76	–
Inhibited	19.99	1.53	65.24	11.10	1.10	1.04

and substrate. Taking into account the expected ratio that is shown between the two S1 peaks [24], and the general X-ray photoelectron spectroscopy survey (not shown) with the elemental composition (Table 3), the data are in good agreement with the EDAX results. The application of the inhibitor to the substrate apparently forms a chemical bond with the substrate and results in a chromium-rich layer at the surface/electrolyte interface.

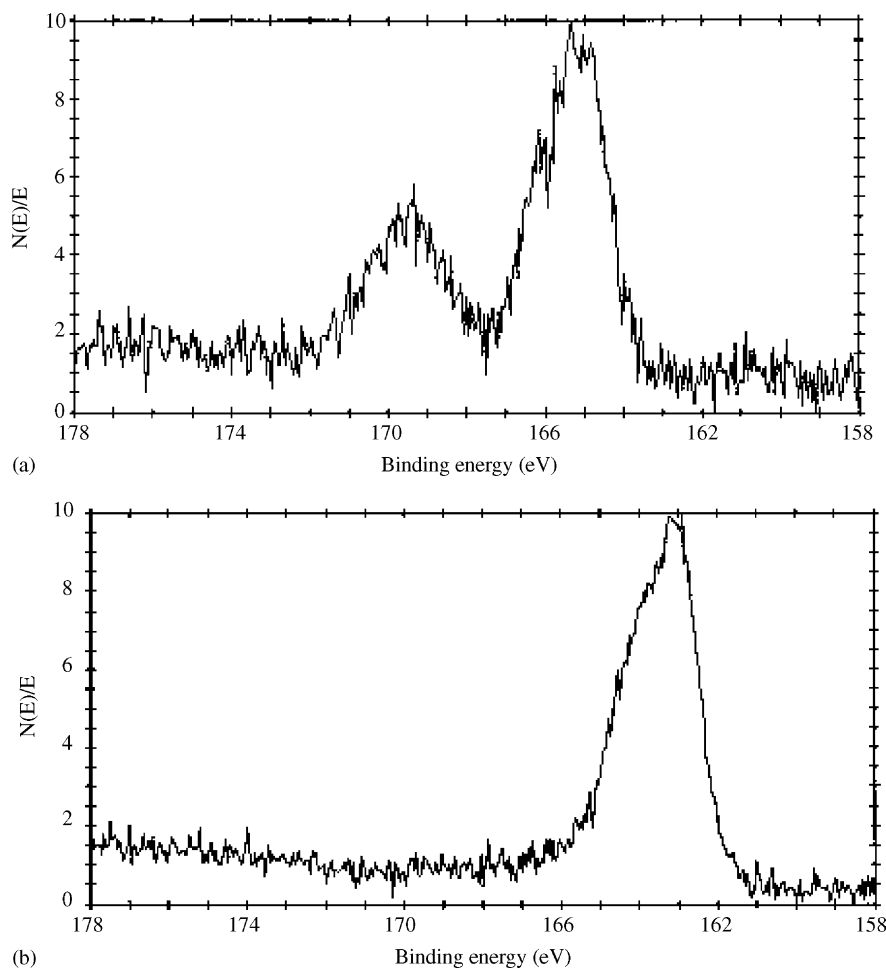


Fig. 10. XPS data of stainless steel samples exposed to the inhibitor (a) and a platinum substrate exposed to the same inhibitor (b).

4. Conclusions

The adsorption of 2-thiophene carboxylic hydrazide follows a Langmuir isotherm and the heats of adsorption range between -57 and -129 kcal mol $^{-1}$. Surface measurements showed that the application of the inhibitor protected the surface by forming a thin layer that forms a chemical bond with the substrate. The extent of surface coverage decreases with temperature as well as the inhibition efficiency. Therefore, thiophene derivatives can be used as inhibitors for stainless steel of type 316 in acidic media with low and moderate concentrations.

Acknowledgements

We would like to express our appreciation to Prof. J.F. Boreo of the University of Cincinnati for allowing us the use of the X-ray photoelectron spectroscopy instrument. We are also grateful to the National Science Foundation (USA), and the Division of Research of the University of Cairo for partial financial assistance.

References

- [1] A.J. Szyprowski, Br. Corros. J. 37 (2002) 141.
- [2] C. Carboni, P. Peyre, G. Beranger, C. Lemaitre, J. Mater. Sci. 37 (2002) 3715.
- [3] M.A. Quraishi, F.A. Ansari, D. Jamal, Mater. Chem. Phys. 77 (2003) 687.
- [4] A. El-Kanouni, S. Kerti, A. Srhiri, K. Bachir, Bull. Electrochem. 12 (1996) 517.
- [5] M.H. Moayed, R.C. Newman, Corros. Sci. 40 (1998) 519.
- [6] J.R. Galvele, J. Electrochem. Soc. 123 (1976) 464.
- [7] A.M. Al-Mayouf, A.K. Al-Ameery, A.A. Al-Suhybani, Corrosion 57 (2001) 614.
- [8] A. Galal, N.F. Atta, M.H.S. Al-Hassan, Mater. Chem. Phys., 2004, in press.
- [9] G.A. Caignan, S.K. Metcalf, E.M. Holt, J. Chem. Cryst. 30 (2000) 415.
- [10] D.H. Gibson, H.Y. He, M.S. Mashuta, Organometallics 20 (2001) 1456.
- [11] D.X. Ren, A.T. Hubbard, J. Colloid Interf. Sci. 202 (1998) 89.
- [12] P. Mills, S. Korlann, M.E. Bussell, M.A. Ovchinnikov, R.J. Angelici, C. Stinner, T. Weber, R. Prins, J. Phys. Chem. A 105 (2001) 4429.
- [13] I.A. Ammar, S. Darwish, Corros. Sci. 7 (1967) 679.
- [14] H. Fisher, Ann. Univ. Ferrara. Sez. 3 (Suppl. 3) (1960) 1.
- [15] J.O.M. Bockris, D. Drazis, Electrochim. Acta 4 (1961) 325.
- [16] G.K. Gomma, M.H. Wahdan, Bull. Chem. Soc. Jpn. 67 (1994) 2621.

- [17] E.J. Kelly, J. Electrochem. Soc. 112 (1965) 124.
- [18] H. Ashassi-Sorkhabi, M.R. Majidi, K. Seyyedi, Appl. Surf. Sci. 225 (2004) 176.
- [19] G. Devarajan, K. Balakrishnan, Bull. Electrochem. 3 (1987) 213.
- [20] S.C. Roy, S.K. Roy, S.C. Sicar, Br. Corros. J. 23 (1988) 2.
- [21] M. Asawa, Corrosion 46 (1990) 823.
- [22] C.I. Cabello, I.L. Botto, H.J. Thomas, Appl. Catal. A 197 (2000) 79.
- [23] M. Jones Jr., Organic Chemistry, W.W. Norton, New York, 2000, p. 651.
- [24] C.D. Wagner, W.M. Riggs, L.E. Davis, J.F. Moulder, in: G.E. Muilenberg (Ed.), Handbook of X-ray Photoelectron Spectroscopy, Perkin Elmer, Minnesota, 1979, p. 80.